m6a Methylation Inhibition by Cycloleucine Impaired Porcine Oocyte Meiosis and Early Embryonic Development via Remodeling Histone Modifications and Altering Metabolism Related Gene Expression in Blastocysts

Meng Zhang
   Jilin University

Sheng Zhang
   Jilin University

Yanhui Zhai
   Jilin University

Yu Han
   Jilin University

Rong Huang
   Jilin University

Xinglan An
   Jilin University

Xiangpeng Dai
   Jilin University

Ziyi Li（✉ Ziyi@jlu.edu.cn ）
   JLU: Jilin University

Research

Abstract

Background

Oocytes maturation and early embryo development were regulated precisely by a series of factors at transcriptional and posttranslational levels. N6-methyladenosine (m^{6}A) is the most prevalent modification in mRNA as a crucial regulator in RNA metabolism and gene regulation. However, the role of m^{6}A on porcine oocyte maturation and early embryogenesis is largely unknown.

Results

Here, we found that oocytes treated with cycloleucine (CL), an inhibitor of m^{6}A, could impair cumulus expansion, elevate mitochondrial reactive oxygen species (ROS) concentration and decreased oocytes maturation which partially caused by disturbed spindle organization and chromosomes alignment. Moreover, our results indicated that the CL treated parthenogenetic embryos arrested at 4-cell stage and showed worse blastocyst quality. CL treatment not only decreased the methylation levels of nucleic acid, H3K4me3 and H3K9me3, while increased the acetylation level of H4K16 during parthenogenetic embryos development in pigs. Furthermore, single cell RNA-seq (scRNA-seq) analysis indicated that CL treatment dramatically elevated the expression of metabolism-related (SLC16A1 and MAIG3 etc.) and maternal related (BTG4, WEE2 and BMP15 etc.) genes at blastocyst stage.

Conclusions

Taken together, we found that m^{6}A methylation inhibition by CL impaired porcine oocyte meiosis and early embryonic development via remodeling histone modifications and altering metabolism related gene expression in blastocysts.

Introduction

The maturation of oocytes is a complex physiological and biochemical process [1]. In mammalian, oocyte maturation is accompanied by meiosis, which is precisely regulated by a series of factors and complex regulatory mechanisms [2, 3]. The matured oocytes initiate early embryonic development once fertilization or parthenogenetic activation. Importantly, epigenetic modifications have been found to play crucial roles during oocyte maturation and early embryonic development [4–7].

As the most common modification on mRNA, N6-methyladenosine (m^{6}A) modification are dynamic and reversible in eukaryotes [8]. In mammals, m^{6}A is regulated by methyltransferase complex (MTC), including methyltransferase like 3 (METTL3), methyltransferase like 14 (METTL14) and Wilms tumor 1-associating protein (WTAP). An increasing number of studies indicated that m^{6}A play crucial roles in disease development [9], stem cell fate determination [10] and early embryonic development [11, 12]. As a major methyl donor in eukaryote, S-adenosylmethionine is synthesised by Methionine adenosyltransferase II (MAT) [13]. However, cycloleucine (1-aminocyclopentane-1-carboxylic acid, CL), a

chemical inhibitor of methionine adenosyltransferase (MAT), could reduce the RNA m^{6}A level [14]. Sun *et al.*, suggested that CL treatment reduced the H3K4me3 level and resulted in embryos development arrest at morula stage in mice [15]. However, the underlying mechanism of CL treatment in regulating porcine embryo development remains largely unknown.

In the present study, we investigated the effect of different concentrations of CL on the porcine oocyte meiotic maturation and subsequent development after parthenogenetic activation (PA). Our finding indicated that CL treatment impaired cumulus expansion and caused aberrant spindle assembly in porcine oocytes. Furthermore, CL treatment altered m^{6}A and histone modification levels which dysregulate the expression of development related genes and subsequently decreased the developmental potency of preimplantation embryo development. Our study may provide new insights into the effect of m^{6}A on porcine oocyte maturation and early embryonic development.

Methods

Antibodies

Mouse monoclonal anti-α-tubulin-FITC antibody was purchased from Sigma (St. Louis, MO, USA). Rabbit polyclonal anti-m^{6}A (202003) was purchased from Synaptic Systems (Goettingen, Germany); Rabbit H3K9me3 (ab8898) and H3K4me3 (ab8580) were purchased from Abcam (Cambridge, MA, USA); Rabbit polyclonal anti-histone H4 (acetyl K16) antibody (ab109463) was purchased from Abcam; Rabbit monoclonal anti-γH2A.X antibody were purchased from Cell Signaling Technology (Danvers, MA, USA); Alexa Fluora 488 goat anti-mouse (A-11001) and Alexa Fluora 594 goat anti-rabbit (A-11037) were purchased from Invitrogen (Invitrogen, MA, USA).

The collection and in vitro maturation (IVM) of porcine oocytes

The porcine ovaries were collected immediately after being slaughtered in a local abattoir, and then were transported to the laboratory within 2 hours in 0.9% NaCl supplemented with 5% penicillin-streptomycin at 35-36.5 °C. COCs (cumulus-oocyte complexes) were collected using a 10 ml syringe from 2−6 mm ovarian follicles. Then the COCs with more than three layers of cumulus cells were selected and cultured in the *in vitro* maturation (IVM) medium. A group of 200 COCs was cultured in 1 mL of maturation medium I (TCM-199 supplemented with 26 mM sodium bicarbonate, 3.05 mM glucose, 0.91 mM sodium pyruvate, 0.5 μg/mL follicle-stimulating hormone (FSH), 0.5 μg/ml luteinizing hormone (LH), 10 ng/ml epidermal growth factor (EGF), 0.1% PVA, 0.03% BSA and 0.1% penicillin/streptomycin) covered with liquid paraffin oil at 38.5 °C with 5% CO_2 for 22−24 h, and then cultured in maturation medium II (the same medium with medium I without hormone) until 42−44 h according to our previous description [16].

The isolation and culture of porcine cumulus cells (CCs)

The CCs were isolated from COCs with 0.2% hyaluronidase, collected by a 15 mL centrifuge tube. After centrifuging at1500 g for 5 min, CCs were resuspended with DMEM/F12 medium (Gibco, Beijing, China),

and subsequently plated onto 60-mm culture plate in DMEM/F12 supplemented with 10% FBS (Gibco, Beijing, China), 100 units/mL penicillin, and 100 μg/mL streptomycin in a humidified atmosphere with 5% (v/v) CO_2 at 37 °C.

Cycloleucine (CL) treatment

In the present study, COCs were cultured in IVM medium supplemented with cycloleucine (CL) (A48105, Sigma) at a concentration of 10, 20, 40 mM, respectively.

Oocytes at Metaphase I (MI) and Metaphase II (MII) stages were collected at 27 h and 42 h, respectively. For cumulus cell (CCs) treatment, CCs were isolated from COCs by 0.2% hyaluronidase and then were treated with CL at a working concentration of 20 mM.

Calculation of area of CCs expansion and viability

Cumulus expansion was measured during the COCs in vitro maturation period, as described previously [17]. Briefly, 40 COCs of each group were taken out of the incubators and captured by a fluorescence microscope. The size of each COC within different groups were measured at 0 h, 24 h and 44 h of *in vitro* maturation. The ImageJ software was used to calculate the area of CCs expansion according with the description previously. The cumulus expansion rate of control group was calculated as 100% at 44 h of *in vitro* maturation, and it was performed at least three times. For the evaluation of cell viability, COCs were digested with 0.2% hyaluronidase [18]. After separating CCs with oocytes, the CCs were staining 0.4% trypan blue solution. Simultaneously, the cell viability was assessed by a light microscope (Nikon, Tokyo, Japan), living cells could not be stained with trypan blue. For oocytes survival rate, oocytes which possess intact zona pellucida and plasma membrane, evenly distributed cytoplasm were regarded as morphological survival. The cell viability was calculated as the percentage of viable cells out of total cells number and it was performed at least three independent replicates.

Parthenogenetic activation (PA) of porcine oocytes

Parthenogenetic activation of porcine oocytes was performed according with the description previously [19]. Briefly, after digestion with 0.2% hyaluronidase for 5 min, denuded MII oocytes (with the first polar) were equilibrated in the activation medium (0.28 M mannitol, 0.5 mM Hepes, 0.1 mM $MgCl_2$, and 1 mM $CaCl_2$) for almost 20 seconds. And then the oocytes were activated by an ECM2001 electro-fusion instrument (ECM2001, BTX, USA) with two direct-current pulses of 1.2 kV/cm for 30 μs. Then the oocytes were cultured in PZM-3 medium (108 mM NaCl, 10 mM KCl, 0.35 mM KH_2PO_4, 0.4 mM $MgSO_4.7H_2O$, 25.07 mM $NaHCO_3$, 0.2 mM Na-pyruvate and 2 mM Ca-lactate.$5H_2O$, 1 mM L-glutamine, 5 mM hypotaurine, 0.3% BSA, 20 mL/L BME amino acid and 10 mL/L MEM non-essential amino acid)) at 38.5 °C with 5% CO_2 for 7 days. The cleavage and blastocyst rates of embryos were visually checked at 48 h and 7 days after PA.

Immunofluorescence (IF) staining

Immunofluorescence staining was performed according with our description previously [20]. Briefly, the oocytes or embryos were removed of zona pellucida with 0.5% acidic Tyrode solution. After washed with PBS/PVA (1 mg/1 mL) for three times, oocytes or embryos were fixed with 4% paraformaldehyde (PFA) for 40 min at room temperature. The samples were permeabilized with 1% Triton-X 100/PBS for 20 min and blocked with 2% BSA/PBS for 1 h at RT. Then the samples were incubated overnight at 4 °C with primary antibodies according to manufacturer's recommended dilutions. After being washed with PBS/PVA for three times, samples were stained with secondary antibodies in the dark for 2 h at 37 °C. Then the DNA was stained with 10 µg/mL DAPI for 15 min. The oocytes or embryos were mounted on coverslips in ProLong Diamond Antifade Mountant reagent (Life Technologies, USA). A fluorescence microscope (Nikon, Tokyo, Japan) was used to capture fluorescent images by setting the same parameters for all groups. The fluorescent images for α-tubulin were taken by a confocal laser-scanning microscope (LSM8800, Zeiss, Oberkochen, Germany). The relative fluorescence intensity was analyzed by Image J software (National Institutes of Health, Bethesda, MD) according to the previous description.

Cell number counting of blastocyst

Total cell numbers of blastocysts were assessed and calculated by staining with Hoechst33342 (10 µg/mL). Briefly, blastocysts were fixed with 4% PFA in PBS/PVA for 40 min, followed by permeabilization in 1% Triton-X 100/PBS for 30 min at RT. After being washed with PBS/PVA for 3 times (5 min/time), the blastocysts were stained with Hoechst33342 for 15 min at RT. Then the blastocysts were mounted on coverslips in ProLong Diamond Antifade Mountant reagent (Life Technologies, USA), and total cell number was observed and counted under a fluorescence microscope (Nikon, Tokyo, Japan).

TUNEL assay

The embryos were removed of zona pellucida with 0.5% acidic Tyrode solution, and permeabilized by 1% Triton-X 100/PBS. After permeabilization, embryos were incubated with TUNEL solution from the In Situ Cell Death Detection Kit (Roche; Mannheim, Germany) in the dark at 37 °C for 1 h. Then, embryos were washed three times with PBS/PVA. DNA were stained with DAPI for 15 min. All samples were observed under a fluorescence microscope (Nikon, Tokyo, Japan) after mounting. Each experiment was biologically replicated at least 5 times. The same exposure times and microscope settings were used for all captured images.

Reactive oxygen species (ROS) generation detection

The ROS level of oocytes were detected by a Reactive Oxygen Species Assay Kit (Beyotime Institute, Shanghai, China) following the manufacturer's instructions. Briefly, 100 denuded oocytes of each group were incubated with dichlorofluorescein diacetate (DCFH-DA) probe (10 µmol/L) in the dark at 38.5 °C for 1 h followed by washing three times with PBS, the oocytes were transferred and mounted on a glass slide, and then were observed with fluorescence microscope (Nikon, Tokyo, Japan) with the same exposure times and microscope settings.

Library preparation and single-cell RNA-seq (scRNA-seq)

The SMART-Seq2 technology was used to detect the global gene expression level in different groups. Briefly, the zona pellucida-free embryos (more than 20 blastomeres) were washed with PBS/PVA, and then were transferred into 0.2 mL tube with 4 μL lysis buffer (including 0.2 μL diluted ERCC spike-in) (1:1000). After SMART amplification, Ampure XP beads were used to purify the cDNA, and Qubit 3.0 Flurometer (Thermo Fisher Scientific, Waltham, MA, USA) was used to measure the concentration of library, Agilent 2100 Bioanalyzer (Agilent Technologies) was used to detect the insert size and quality of amplified library. All libraries (PACL_4cell, PA_4cell, PACL_Bla and PA_Bla) were sequenced by Annoroad Biotechnology (Beijing, China) on an Illumina platform, and generated 150 bp paired-end reads. The clean reads were mapped to Sus_scrofa. Sscrofa11.1 and quantified gene expression levels as TPM (Transcripts Per Million).

Identifying differentially expressed genes (DEGs) and lncRNAs (DElncRNAs)

DESeq2 was used for DEGs and DELncRNAs analysis of RNA-seq with a threshold of false discovery rate (FDR) < 0.05 and |log2FC| >1 between two groups.

Co-expression and Function analysis

The DEGs, target genes of DElncRNAs were performed function enrichment analysis, including GO and KEGG signaling pathway analysis using KOBAS 3.0 software. The lncRNAs-gene interaction networks were visualized with Cytoscape 3.4.0 (http://www.cytoscape.org/).

Predication of m^{6}A sites in mRNA

The m^{6}A sites of genes were predicated with the online software SRAMP (http://www.cuilab.cn/sramp) with default parameters. The very high/high/moderate confidence m^{6}A sites were considered as the predicted m^{6}A sites.

RNA isolation and real-time quantitative PCR (qRT-PCR)

Total RNA was isolated from porcine oocyte or embryos with RNeasy Mini Kit (Qiagen, Hilden, Germany) according to the manufacturer's instructions. cDNA was synthesis by Transcript All-in-one First-Strand cDNA Kit (TransGen, Beijing, China), followed by qRT-PCR on a StepOnePlus™ Real-time PCR systems instrument (Applied Biosystems). The qPCR primers were designed by Primer3plus (http://primer3.sourceforge.net/webif.php) and synthesized by Comate biotech Co., Ltd. (Changchun, Jilin, China) (Table S1). In the present study, GAPDH was used as the internal control gene. The $2^{-\Delta\Delta Ct}$ method was used for the calculation of gene relative abundance.

Statistical analysis

All experiments were performed at least three independent replicates. GraphPad Prism8 statistical software (Graphpad Software, San Diego, CA, USA) was used for data analysis. Graphics were drawn using GraphPad Prism8 and R software (4.0). The results were presented as Mean ± SEM, and analyzed

by t-test, one-way ANOVA test and multiple t test. $p < 0.05$ was considered statistically significant, $p < 0.01$ was considered extremely significant.

Results

m^6A methylation inhibition by CL treatment impaired oocyte quality and expansion of CCs via altering the m^6A level

To investigate the effect of MAT inhibitor on porcine oocyte maturation, the COCs were cultured in different concentration of CL (10 mM, 20 mM and 40 mM) for 44 h at 38.5 °C and the survival rate and maturation rate were evaluated (Fig. 1a, and 1b). Our results showed that both the survival rate and maturation rate of oocyte in 10 mM, 20 mM, 40 mM CL group were significantly decreased ($p < 0.01$) (Fig. 1a, and 1b). The IF immunostaining analysis of m^6A revealed that m^6A was present both in the cytoplasm and nucleus (Fig. 1c). 20 mM CL treated oocytes displayed a markedly reduced m^6A signal ($p < 0.01$), which was further confirmed by the fluorescence intensity result of m^6A (Fig. 1d).

In addition, we assessed the condition of cumulus cells (CCs) surrounding the oocytes during maturation (Fig. 2a). Results showed that the survival rates of CCs treated with CL (20 mM) were remarkably decreased at 24 h and 44 h of *in vitro* maturation compared with control group ($p < 0.01$) (Fig. 2b). Moreover, the expansion rate of CCs in the CL group was significantly lower than that of control group at 24 h and 44 h of *in vitro* maturation ($p < 0.01$) (Fig. 2c). Furthermore, the m^6A level of CCs was detected by immunostaining and the m^6A signal in CL treated-CCs was significantly decreased (Fig. 2d), which was consist with the result of fluorescence intensity ($p < 0.01$) (Fig. 2e). Interestingly, our qRT-PCR assay results indicated that exposure to CL inhibited the expression of CCs expansion-related genes EFNB2, HAS2, PTX3 and antiapoptotic proteins BCL2 ($p < 0.05$) and promoted the expression levels of apoptosis-related genes BAX and P53 ($p < 0.01$) (Fig. 2f and 2 g).

m^6A methylation inhibition by CL treatment caused aberrant spindle assembly and oxidative stress in porcine oocytes

Given the importance of spindle assembly in meiosis, next we sought to examine the spindle/chromosome structure in porcine oocytes after CL treatment. As showed in Fig. 3e, the control oocytes at MI stage showed a normal barrel-shape spindle with well- aligned chromosomes at the equatorial plate, while CL treated oocytes showed disorganized spindle and misaligned chromosome (Fig. 3a). The abnormal rates of spindle/chromosome structure were considerably higher in CL-treated oocytes than in

the control group (Fig. 3b). Previous studies suggested that m^6A was associated with oxidative stress which can impede oocyte maturation and embryonic development [21, 22]. To investigate whether the CL would induce oxidative stress in oocyte, we next examined the relative ROS level in oocyte with DCFH-DA probes. Our result showed that the ROS level of CL-treated oocytes was significantly higher than that of

control group ($p < 0.01$) (Fig. 3c), which was confirmed by the fluorescence intensity result ($p < 0.01$) (Fig. 3d).

m^{6}A methylation inhibition by CL treatment decreased early developmental potency of parthenogenetic embryos

To investigate whether the treatment of CL will exert a long-term effect on oocytes, we then analyzed the development ability of embryos produced by PA (Fig. 4a). The MII oocytes were selected and subjected to PA, and then the PA oocytes were cultured with CL (20 mM) exposure or control in PZM medium. Our results showed that the rates of cleavage and blastocyst were significantly decreased in CL group when compared with control group ($p < 0.01$) (Fig. 4b). Furthermore, the apoptosis analysis result suggested that the cell apoptotic signal (TUNEL) was considerably high in CL-treated blastocysts when compared with control group (Fig. 5a). Moreover, a massive accumulation of γH2A.X foci on the DNA were observed in CL-treated embryos ($p < 0.01$) (Fig. 5b) which was confirmed by fluorescence intensity ($p < 0.01$) (Fig. 5c and 5d). Subsequently, the blastocyst quality was assessed and our results indicated that the diameter and cell number of blastocysts were significantly reduced in CL-treated blastocysts ($p < 0.01$) (Fig. 5g and 5 h). Furthermore, qRT-PCR result showed that CL treatment significantly decreased the mRNA levels of pluripotency genes NANOG and OCT4 at 2cell, 4cell and blastocyst (Bla) stage ($p < 0.01$) (Fig. 5i). Moreover, apoptotic-related genes BCL2 was significantly downregulated at stage of blastocyst ($p < 0.05$), while the mRNA level of anti-apoptosis gene BAX was significantly upregulated during embryonic development ($p < 0.05$) (Fig. 5i).

m^{6}A methylation inhibition by CL treatment reduced the RNA m^{6}A methylation during PA embryogenesis

Given that CL inhibits the catalytic of MAT2A and subsequently affects SAM level in eukaryotes, we then detected the mRNA expression level of methyltransferases (METTL3, METTL14 and WTAP) and nucleic acid methylation during embryogenesis by immunofluorescence staining. The qRT-PCR result showed that the transcript level of METTL3 was significantly increased at the 4-cell and 8-cell stage, while decreased at blastocyst stage compared with control group (Fig. 6a). The expression of methyltransferase METTL14 was significantly downregulated at 4-cell while upregulated at 8-cell and blastocyst stage (Fig. 6a). However, WTAP mRNA level was decreased at 2-cell, 4-cell and blastocyst stage (Fig. 6a). Interestingly, the m^{6}A level was significantly decreased at 2-cell, 4-cell and blastocyst stage ($p < 0.01$) (Fig. 6b and 6c).

m^{6}A methylation inhibition by CL treatment remodels histone modification during embryogenesis

Recently studies also reported that there is crosstalk between m^{6}A and histone modifications, which play vital role in embryo development [5, 23–25]. We then sought to investigate whether the CL treatment could lead to some change of histone modification during embryonic development which subsequently affect the embryo development. Firstly, we examined the methylation status of H3K9 and H3K4 by immune-staining after CL treatment during PA embryogenesis. The results indicated that the level of H3K9me3 was dramatically decreased in CL treated embryos at 4-cell and blastocyst stage as compared with control ($p < 0.01$) (Fig. 7a and 7b). Compared with control, the level of H3K4me3 was significantly decreased in CL treated embryos at 2-cell, 4-cell and blastocyst stage ($p < 0.05$) (Fig. 7c and 7d). In contrast, the level of H4K16ac was significantly upregulated at the 2-cell, 4-cell and blastocyst stage compared with control group ($p < 0.05$) (Fig. 7e and 7f).

m^{6}A methylation inhibition by CL treatment altered the global transcriptome of early embryos

Previous study suggested that epigenetic modification has notable effects on gene expression [5, 6, 23]. To investigate the gene expression profile of embryos after CL treatment, embryos treated with or without CL were collected at 4-cell and blastocyst stage and used for scRNA-seq (Fig. 8a). The correlation analysis between samples indicated that the difference between 4-cell and blastocyst was bigger than the difference between CL exposure and control (Fig. 8b). A total of 22, 682, 14352 and 13603 differently expressed (DE) genes between different groups (PACL_4cell-vs-PA_4cell, PACL_Bla-vs-PA_Bla, PACL_Bla-vs-PACL_4cell and PA_Bla-vs-PA_4cell) were identified in the present study (Fig. 8c), and the intersection of DE genes between different groups were shown in Venn diagram (Fig. 8d). In addition, we compared the global transcripts level between different groups. As illustrated in Fig. 9e, the global gene expression level was dramatically increased after CL treatment at the 4-cell and blastocyst stage of PA embryos ($p < 0.001$).

To exclude the effect of m^{6}A on the DE genes expression, we then analyzed the potential m^{6}A sites in the top twelve DE genes. The result showed that most of the DE genes have more than one moderate-confidence m^{6}A site (Fig. 9a). Functional analysis result suggested that these DE genes mainly enriched on Protein processing in endoplasmic reticulum, P53 signalling pathway, Lysosome pathway and several metabolism-related pathways (Fig. 9b). Moreover, we also analyzed the DE lncRNAs in the present study. We got 28, 237, 6651 and 7215 DE lncRNAs between different groups (PACL_4cell-vs-PA_4cell, PACL_Bla-vs-PA_Bla, PACL_Bla-vs-PACL_4cell and PA_Bla-vs-PA_4cell), respectively. Co-expression analysis suggested that these DE lncRNAs were significantly correlated with DE genes at 4-cell and blastocyst stage of PA embryos. We finally constructed lncRNA-mRNA networks based on the integrated analysis of lncRNA/mRNAs co-expression and target gene prediction (Fig. 9f and 9 g). Noticeably, NONSUSTOO3873.1 and NONSUST017827.1 have the top degree of the network at 4-cell and blastocyst stage, respectively (Fig. 9f and 9 g).

Discussion

Oocytes quality is closely related to fertilization and early embryonic development [26, 27]. It is widely believed that high quality mature oocyte is usually characterized by some typical features, such as the well-organized CCs [28], high-proportioned oocyte survival rate [18] and first polar body extrusion rate [29]. The communication between the oocyte and its surrounding CCs is essential for oocyte development and granulosa cell differentiation [30, 31]. A growing number of studies indicated that m^{6}A play crucial roles in the development of reproductive organ [32], gametogenesis [33], fertilization [34] and early embryonic development [7, 35]. Cao *et al.* found that there exist abundant m^{6}A modification sites in genes for porcine granulosa cells [36]. The differentially expressed m^{6}A methylated genes were significantly enriched in several signaling pathways related with steroidogenesis, granulosa cell proliferation and follicular development [36]. Wang *et al.*, reported that CL treatment impaired the maturation of porcine oocytes and reducing the RNA m^{6}A level [37]. However, little is known about the effect of RNA m^{6}A on the CCs expansion and ROS level of porcine oocytes. In our present study, we found that CL exposure significantly decreased the expansion of CCs and oocyte maturation via repressing the RNA m^{6}A level. Meanwhile, the ROS level were dramatically increased in CL-treated oocytes. Taken together, CL reduced the m^{6}A level, resulted in abnormal CCs expansion and ROS accumulation and spindle morphology and chromosome alignment.

Except for oocyte maturation, RNA m^{6}A modification has been found to play notable effects on embryonic development [12, 38]. In mice, CL exposure resulted in embryos arrested at morula stage [15]. In our study, CL treatment impaired the cleavage, blastocyst rates and total cell number of parthenogenetic embryos in pigs. We speculate that the endogenous m^{6}A level might lead to different effects of CL on embryonic development in various mammals. Notably, Sun *et al.*, found that CL reduced the H3K4me3 abundance in the mouse embryos treated with CL [15]. In the present study, we found that both the H3K4me3 and H3K9me3 levels were dramatically decreased in CL-treated medium during embryonic development in pigs. In addition, the level of H4K16ac was increased during parthenogenetic embryogenesis when treated with CL, indicating that crosstalk between m^{6}A and histone modifications during embryonic development. Moreover, the DNA damage signal (γH2A.X) was significantly increased at the blastocyst stage in CL-treated group, suggesting that DNA damage caused by m^{6}A decrease might further impaired embryonic development.

To further clarify the potential genes regulated by m^{6}A during embryonic development, we compared the global transcript levels at the stage of 4-cell and blastocyst. RNA-seq analysis suggested that CL treatment dramatically changed the transcript levels of large number of genes and lncRNAs at blastocyst stage, while only several DE genes and lncRNAs were identified at 4-cell stage. In mouse, Mendel *et al.*, suggested that the downregulated SAM synthetase might trigger massive alteration in gene expression in the blastocysts [39]. We speculate that CL exposure may result in dysregulation of protein levels but not mRNA levels at 4-cell stage during parthenogenetic embryo development, which need to be further confirmed in the further. Notably, SLC16A1, MAGI3, BTG4, WEE2 and DNMT1 have more than five potential m^{6}A sites in their mRNA, indicating that they might be potential target genes affected by m^{6}A during porcine early embryogenesis. The dysregulated expression of SLC16A1 and MAGI3, which can

affect the pyruvate and lactic acid metabolism, may regulate metabolism homeostasis during early embryonic development [40–43]. Notably, several maternal mRNAs such as maternal-to-zygotic transition (MZT) licensing factor BTG4 [44, 45], cell-cycle proteins WEE2 [46] and BMP15 [47] were also identified as DE genes in the present study, suggesting that the RNA m^{6}A modification of these genes may regulate their expression thus participating embryonic development. In addition, little studies focus on m^{6}A-mediated lncRNAs during porcine embryonic development. Our result found the candidate lncRNAs NONSUST017827.1, NONSUST026375.1, NONSUST028825.1 and NONSUST021739.1 may target the metabolism- and embryonic development-related genes thus participating in embryonic development in pigs.

Conclusions

Taken together, our finding found that CL treatment could impair oocytes maturation and early embryonic development via reducing the nucleic acid methylation and histone modification levels. The reduced m^{6}A methylation result in dysregulated expression of lncRNAs, metabolism-related (eg., SLC16A1 and MAGI3) and maternal mRNAs (eg., BTG4, WEE2 and BMP15) at blastocyst thus affecting early embryonic development (Fig. 10). Our findings provide new insights of the regulated roles of RNA m^{6}A modification during embryonic development in mammals.

Abbreviations

Germinal vesicle, GV; Germinal vesicle breakdown, GVBD; Cumulus-oocyte complexes, COCs; Cumulus cells, CCs; Meiosis stage I, MI; Metaphase stage II, MII; Polar body, PB; *In vitro* maturation, IVM; Parthenogenetic activation, PA; Blastocyst, Bla; Cycloleucine, CL; m^{6}A, N6-methyladenosine; 5-methylcytosine, 5mC; 5-hydroxymethylcytosine, 5hmC; Histone H3 trimethylated on Lysine 4, H3K4me3; Histone H3 trimethylated on Lysine 9, H3K9me3; Histone H4 Lysine 16 Acetylation, H4K16Ac; Reactive oxygen species, ROS; methyltransferase like 3, METTL3; methyltransferase-like 14, METTL14. Maternal-to-zygotic transition, MZT.

Declarations

Acknowledgements

Authors' contributions

ZYL designed and coordinated the study. MZ performed immunostaining and embryo culture. MZ wrote the paper. MZ and RH collected scRNA-seq samples, performed the RT-qPCR and taken pictures with the confocal laser microscope. YHL performed western blot. SZ, YHZ and XLA provided technical assistance

and contributed to the data analysis. YH and XPD revised the manuscript. All authors reviewed the results and approved the final version of the manuscript.

Funding

Availability of data and materials

Sequencing data were deposited into NCBI Gene Expression Omnibus (SRA) database with accession numbers SRP289412.

Ethics approval and consent to participate

Not applicable.

Consent for publication

Not applicable.

Competing interests

The authors declare that they have no competing interests.

References

1. Hassold T, Hunt P. To err (meiotically) is human: the genesis of human aneuploidy. *Nat Rev Genet* 2001, 2(4):280-291.
2. Eppig JJ. Coordination of nuclear and cytoplasmic oocyte maturation in eutherian mammals. *Reprod Fertil Dev* 1996, 8(4):485-489.
3. Van den Hurk R, Zhao J. Formation of mammalian oocytes and their growth, differentiation and maturation within ovarian follicles. *Theriogenology* 2005, 63(6):1717-1751.
4. Lu Y, Dai X, Zhang M, Miao Y, Zhou C, Cui Z, Xiong B. Cohesin acetyltransferase Esco2 regulates SAC and kinetochore functions via maintaining H4K16 acetylation during mouse oocyte meiosis. *Nucleic Acids Res* 2017, 45(16):9388-9397.

5. Dahl JA, Jung I, Aanes H, Greggains GD, Manaf A, Lerdrup M, et al. Broad histone H3K4me3 domains in mouse oocytes modulate maternal-to-zygotic transition. *Nature* 2016, 537(7621):548-552.

6. Guo F, Li X, Liang D, Li T, Zhu P, Guo H, et al. Active and passive demethylation of male and female pronuclear DNA in the mammalian zygote. *Cell Stem Cell* 2014, 15(4):447-459.

7. Ivanova I, Much C, Di Giacomo M, Azzi C, Morgan M, Moreira PN, et al. The RNA m(6)A Reader YTHDF2 Is Essential for the Post-transcriptional Regulation of the Maternal Transcriptome and Oocyte Competence. *Mol Cell* 2017, 67(6):1059-1067 e1054.

8. Shi H, Wei J, He C. Where, When, and How: Context-Dependent Functions of RNA Methylation Writers, Readers, and Erasers. *Mol Cell* 2019, 74(4):640-650.

9. Deng X, Su R, Weng H, Huang H, Li Z, Chen J. RNA N(6)-methyladenosine modification in cancers: current status and perspectives. *Cell Res* 2018, 28(5):507-517.

10. Batista PJ, Molinie B, Wang J, Qu K, Zhang J, Li L, et al. m(6)A RNA modification controls cell fate transition in mammalian embryonic stem cells. *Cell Stem Cell* 2014, 15(6):707-719.

11. Zhang M, Zhai Y, Zhang S, Dai X, Li Z. Roles of N6-Methyladenosine (m(6)A) in Stem Cell Fate Decisions and Early Embryonic Development in Mammals. *Front Cell Dev Biol* 2020, 8:782.

12. Sui X, Hu Y, Ren C, Cao Q, Zhou S, Cao Y, et al. METTL3-mediated m(6)A is required for murine oocyte maturation and maternal-to-zygotic transition. *Cell Cycle* 2020, 19(4):391-404.

13. Lin DW, Chung BP, Kaiser P. S-adenosylmethionine limitation induces p38 mitogen-activated protein kinase and triggers cell cycle arrest in G1. *J Cell Sci* 2014, 127(Pt 1):50-59.

14. Wang X, Zhu L, Chen J, Wang Y. mRNA m(6)A methylation downregulates adipogenesis in porcine adipocytes. *Biochem Biophys Res Commun* 2015, 459(2):201-207.

15. Sun H, Kang J, Su J, Zhang J, Zhang L, Liu X, et al. Methionine adenosyltransferase 2A regulates mouse zygotic genome activation and morula to blastocyst transitiondagger. *Biol Reprod* 2019, 100(3):601-617.

16. Zhang Z, Zhai Y, Ma X, Zhang S, An X, Yu H, et al. Down-Regulation of H3K4me3 by MM-102 Facilitates Epigenetic Reprogramming of Porcine Somatic Cell Nuclear Transfer Embryos. *Cell Physiol Biochem* 2018, 45(4):1529-1540.

17. Ralph JH, Telfer EE, Wilmut I. Bovine cumulus cell expansion does not depend on the presence of an oocyte secreted factor. *Mol Reprod Dev* 1995, 42(2):248-253.

18. Yin C, Liu J, Chang Z, He B, Yang Y, Zhao R. Heat exposure impairs porcine oocyte quality with suppressed actin expression in cumulus cells and disrupted F-actin formation in transzonal projections. *J Anim Sci Biotechnol* 2020, 11:71.

19. Hou X, Liu J, Zhang Z, Zhai Y, Wang Y, Wang Z, et al. Effects of cytochalasin B on DNA methylation and histone modification in parthenogenetically activated porcine embryos. *Reproduction* 2016, 152(5):519-527.

20. Zhai Y, Zhang Z, Yu H, Su L, Yao G, Ma X, et al. Dynamic Methylation Changes of DNA and H3K4 by RG108 Improve Epigenetic Reprogramming of Somatic Cell Nuclear Transfer Embryos in Pigs. *Cell*

Physiol Biochem 2018, 50(4):1376-1397.

21. Dennery PA. Effects of oxidative stress on embryonic development. *Birth Defects Res C Embryo Today* 2007, 81(3):155-162.

22. Shi Y, Fan S, Wu M, Zuo Z, Li X, Jiang L, *et al.* YTHDF1 links hypoxia adaptation and non-small cell lung cancer progression. *Nat Commun* 2019, 10(1):4892.

23. Wang C, Liu X, Gao Y, Yang L, Li C, Liu W, et al. Reprogramming of H3K9me3-dependent heterochromatin during mammalian embryo development. *Nat Cell Biol* 2018, 20(5):620-631.

24. Huang H, Weng H, Zhou K, Wu T, Zhao BS, Sun M, et al. Histone H3 trimethylation at lysine 36 guides m(6)A RNA modification co-transcriptionally. *Nature* 2019, 567(7748):414-419.

25. Li Y, Xia L, Tan K, Ye X, Zuo Z, Li M, et al. N(6)-Methyladenosine co-transcriptionally directs the demethylation of histone H3K9me2. *Nat Genet* 2020, 52(9):870-877.

26. Schatten H, Sun QY. Centrosome dynamics during mammalian oocyte maturation with a focus on meiotic spindle formation. *Mol Reprod Dev* 2011, 78(10-11):757-768.

27. Schatten H, Sun QY. Centrosome and microtubule functions and dysfunctions in meiosis: implications for age-related infertility and developmental disorders. *Reprod Fertil Dev* 2015, 27(6):934-943.

28. Appeltant R, Somfai T, Santos ECS, Dang-Nguyen TQ, Nagai T, Kikuchi K. Effects of vitrification of cumulus-enclosed porcine oocytes at the germinal vesicle stage on cumulus expansion, nuclear progression and cytoplasmic maturation. *Reprod Fertil Dev* 2017, 29(12):2419-2429.

29. Jia L, Li J, He B, Jia Y, Niu Y, Wang C, et al. Abnormally activated one-carbon metabolic pathway is associated with mtDNA hypermethylation and mitochondrial malfunction in the oocytes of polycystic gilt ovaries. *Sci Rep* 2016, 6:19436.

30. Russell DL, Gilchrist RB, Brown HM, Thompson JG. Bidirectional communication between cumulus cells and the oocyte: Old hands and new players? *Theriogenology* 2016, 86(1):62-68.

31. Macaulay AD, Gilbert I, Scantland S, Fournier E, Ashkar F, Bastien A, et al. Cumulus Cell Transcripts Transit to the Bovine Oocyte in Preparation for Maturation. *Biol Reprod* 2016, 94(1):16.

32. Zheng G, Dahl JA, Niu Y, Fedorcsak P, Huang CM, Li CJ, et al. ALKBH5 is a mammalian RNA demethylase that impacts RNA metabolism and mouse fertility. *Mol Cell* 2013, 49(1):18-29.

33. Qi ST, Ma JY, Wang ZB, Guo L, Hou Y, Sun QY. N6-Methyladenosine Sequencing Highlights the Involvement of mRNA Methylation in Oocyte Meiotic Maturation and Embryo Development by Regulating Translation in Xenopus laevis. *J Biol Chem* 2016, 291(44):23020-23026.

34. Lin Z, Hsu PJ, Xing X, Fang J, Lu Z, Zou Q, et al. Mettl3-/Mettl14-mediated mRNA N(6)-methyladenosine modulates murine spermatogenesis. *Cell Res* 2017, 27(10):1216-1230.

35. Meng TG, Lu X, Guo L, Hou GM, Ma XS, Li QN, et al. Mettl14 is required for mouse postimplantation development by facilitating epiblast maturation. *FASEB J* 2019, 33(1):1179-1187.

36. Cao Z, Zhang D, Wang Y, Tong X, Avalos LFC, Khan IM, et al. Identification and functional annotation of m6A methylation modification in granulosa cells during antral follicle development in pigs. *Anim*

Reprod Sci 2020, 219:106510.

37. Wang YK, Yu XX, Liu YH, Li X, Liu XM, Wang PC, et al. Reduced nucleic acid methylation impairs meiotic maturation and developmental potency of pig oocytes. *Theriogenology* 2018, 121:160-167.

38. Deng M, Chen B, Liu Z, Cai Y, Wan Y, Zhang G, et al. YTHDF2 Regulates Maternal Transcriptome Degradation and Embryo Development in Goat. *Front Cell Dev Biol* 2020, 8:580367.

39. Mendel M, Chen KM, Homolka D, Gos P, Pandey RR, et al. Methylation of Structured RNA by the m(6)A Writer METTL16 Is Essential for Mouse Embryonic Development. *Mol Cell* 2018, 71(6):986-1000 e1011.

40. Zhang J, Zhao J, Dahan P, Lu V, Zhang C, Li H, et al. Metabolism in Pluripotent Stem Cells and Early Mammalian Development. *Cell Metab* 2018, 27(2):332-338.

41. Pierre K, Pellerin L. Monocarboxylate transporters in the central nervous system: distribution, regulation and function. *J Neurochem* 2005, 94(1):1-14.

42. Ni TK, Elman JS, Jin DX, Gupta PB, Kuperwasser C. Premature polyadenylation of MAGI3 is associated with diminished N(6)-methyladenosine in its large internal exon. *Sci Rep* 2018, 8(1):1415.

43. Weng Q, Chen M, Yang W, Li J, Fan K, Xu M, et al. Integrated analyses identify miR-34c-3p/MAGI3 axis for the Warburg metabolism in hepatocellular carcinoma. *FASEB J* 2020, 34(4):5420-5434.

44. Yu C, Ji SY, Sha QQ, Dang Y, Zhou JJ, Zhang YL, et al. BTG4 is a meiotic cell cycle-coupled maternal-zygotic-transition licensing factor in oocytes. *Nat Struct Mol Biol* 2016, 23(5):387-394.

45. Liu Y, Lu X, Shi J, Yu X, Zhang X, Zhu K, et al. BTG4 is a key regulator for maternal mRNA clearance during mouse early embryogenesis. *J Mol Cell Biol* 2016, 8(4):366-368.

46. Han SJ, Chen R, Paronetto MP, Conti M. Wee1B is an oocyte-specific kinase involved in the control of meiotic arrest in the mouse. *Curr Biol* 2005, 15(18):1670-1676.

47. Chi D, Zeng Y, Xu M, Si L, Qu X, Liu H, et al. LC3-Dependent Autophagy in Pig 2-Cell Cloned Embryos Could Influence the Degradation of Maternal mRNA and the Regulation of Epigenetic Modification. *Cell Reprogram* 2017, 19(6):354-362.
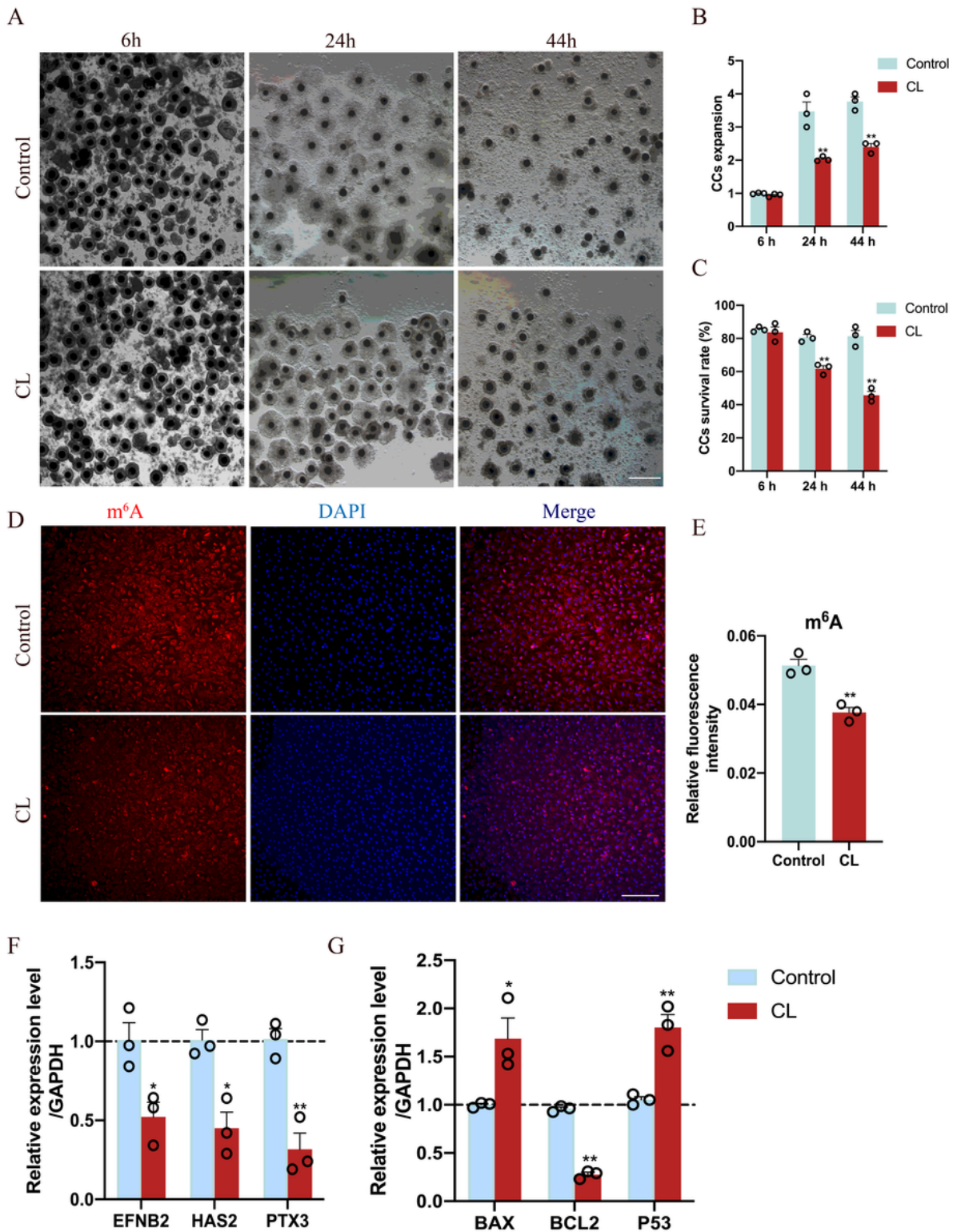
Figures
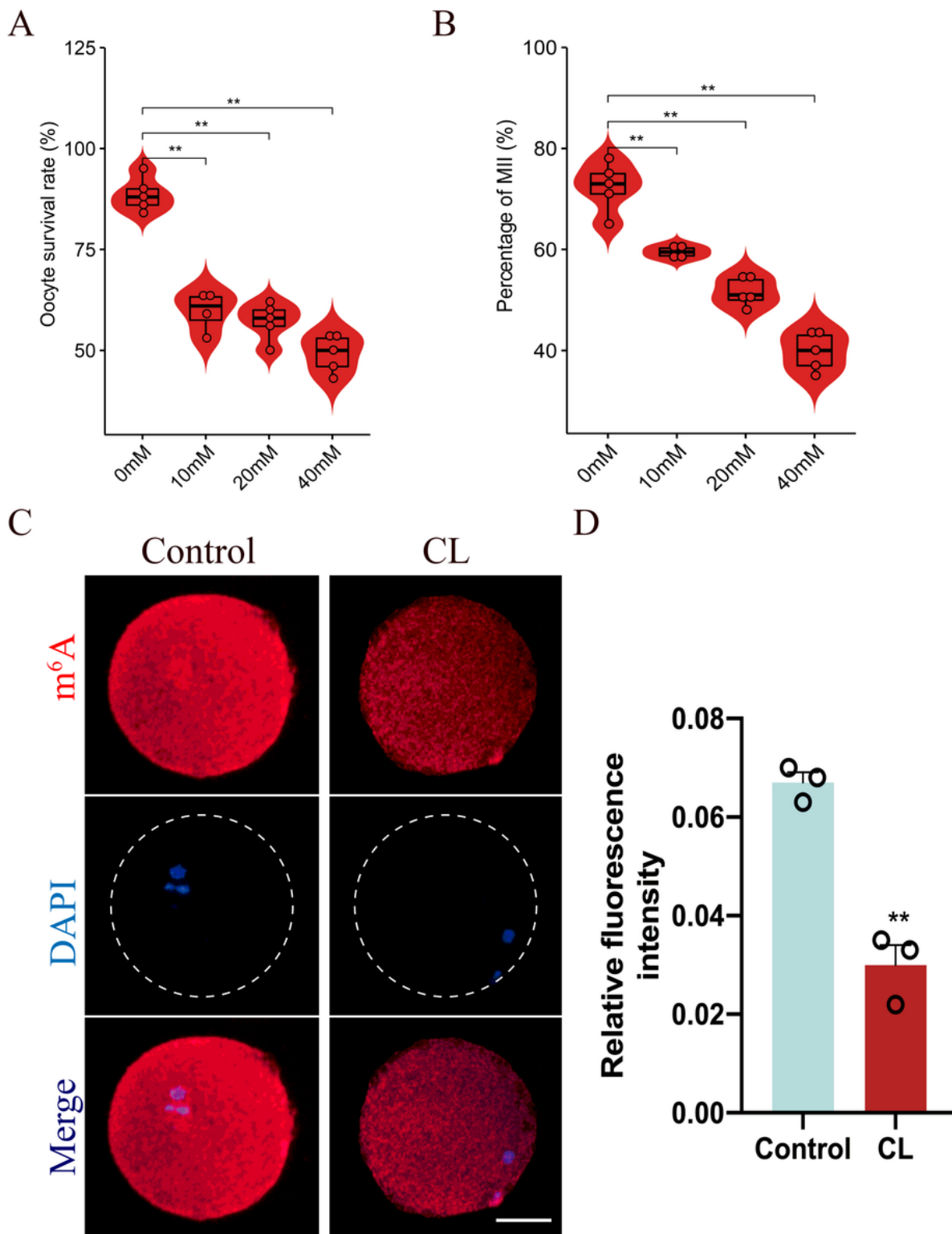
Figure 1

Effects of different doses of CL on the porcine oocyte maturation. (a) Survival rate of CL (0 mM, 10 mM, 20 mM and 40 mM) treated oocytes. (b) The rate of polar body extrusion was recorded in different groups. (c) Representative staining images of m6A in control and CL-treated MII oocytes. Scale bar, 500 μm. (d) The fluorescence intensity of m6A. Data are expressed as mean ± SEM of three independent experiments. * $p < 0.05$, ** $p < 0.01$.
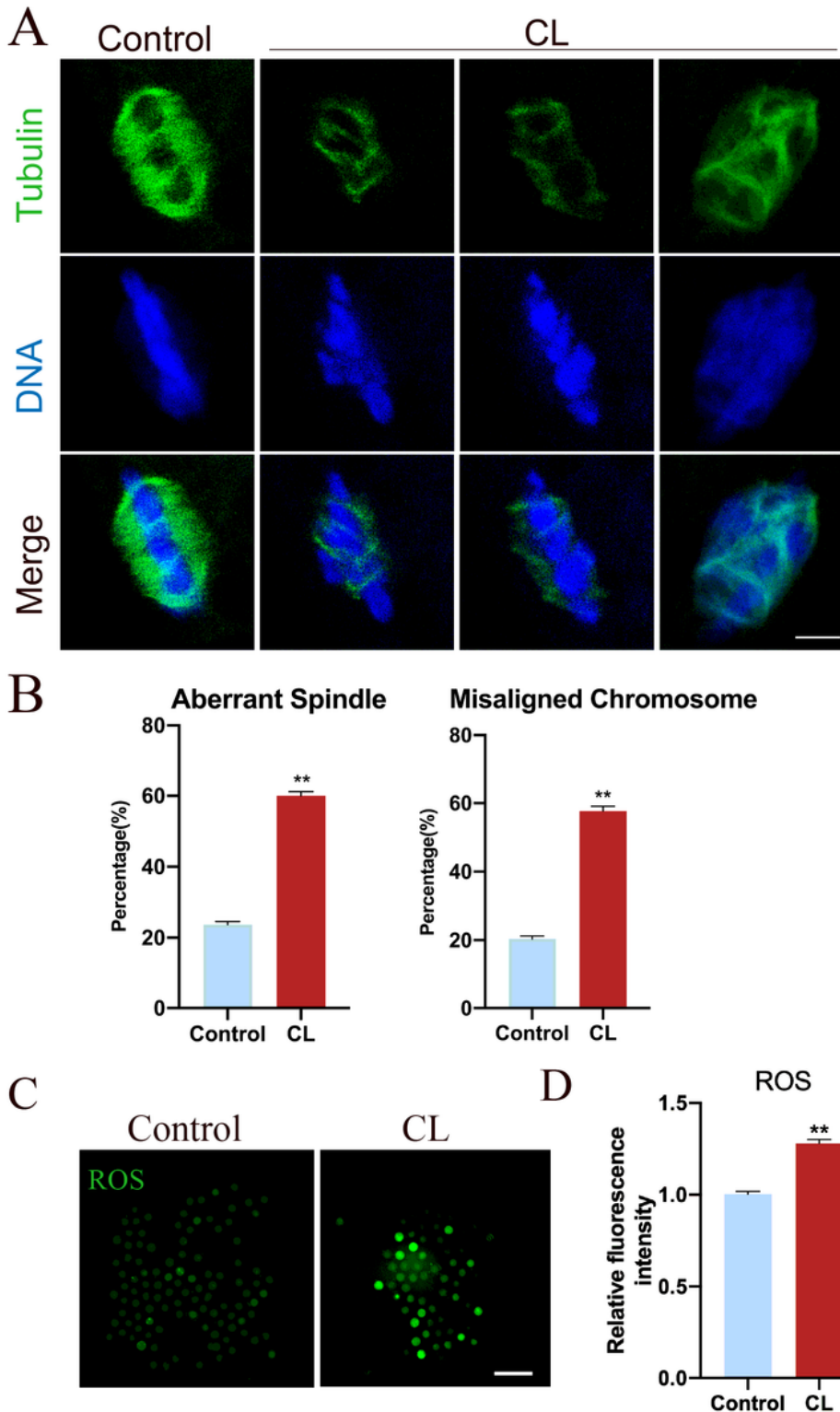
Figure 2

Effects of different doses of CL on the porcine CCs expansion. (a) Representative images of CCs expansion at different stages of in vitro maturation in control and CL-treated COCs. (b) The statistical analysis of CCs survival rates and (c) expansion degree at different stages of in vitro maturation in control and CL-treated COCs. (d) Representative images of m6A in control and CL-treated CCs. Scale bar, 100 µm. (e) The fluorescence intensity of m6A in control and CL-treated CCs. (f) The relative mRNA

expression levels of CCs expansion-related genes and cell apoptosis-related genes in two groups. Data are expressed as mean ± SEM of three independent experiments. * $p < 0.05$, ** $p < 0.01$.

Figure 3

The CL treatment caused abnormal spindle assembly and misaligned chromosome and increased ROS level in porcine oocytes. (a) Representative images of spindle morphologies and chromosome alignment in control and CL-treated oocytes. Scale bar, 5 μm. (b) The rate of aberrant spindles and (b) misaligned

chromosome were recorded in control and CL-treated oocytes. (d) Representative images of ROS level in control and CL-treated oocytes. Scale bar, 100 μm. (d) The fluorescence intensity of ROS level in control and CL-treated oocytes. Data are expressed as mean ± SEM of three independent experiments. * $p < 0.05$, ** $p < 0.01$.
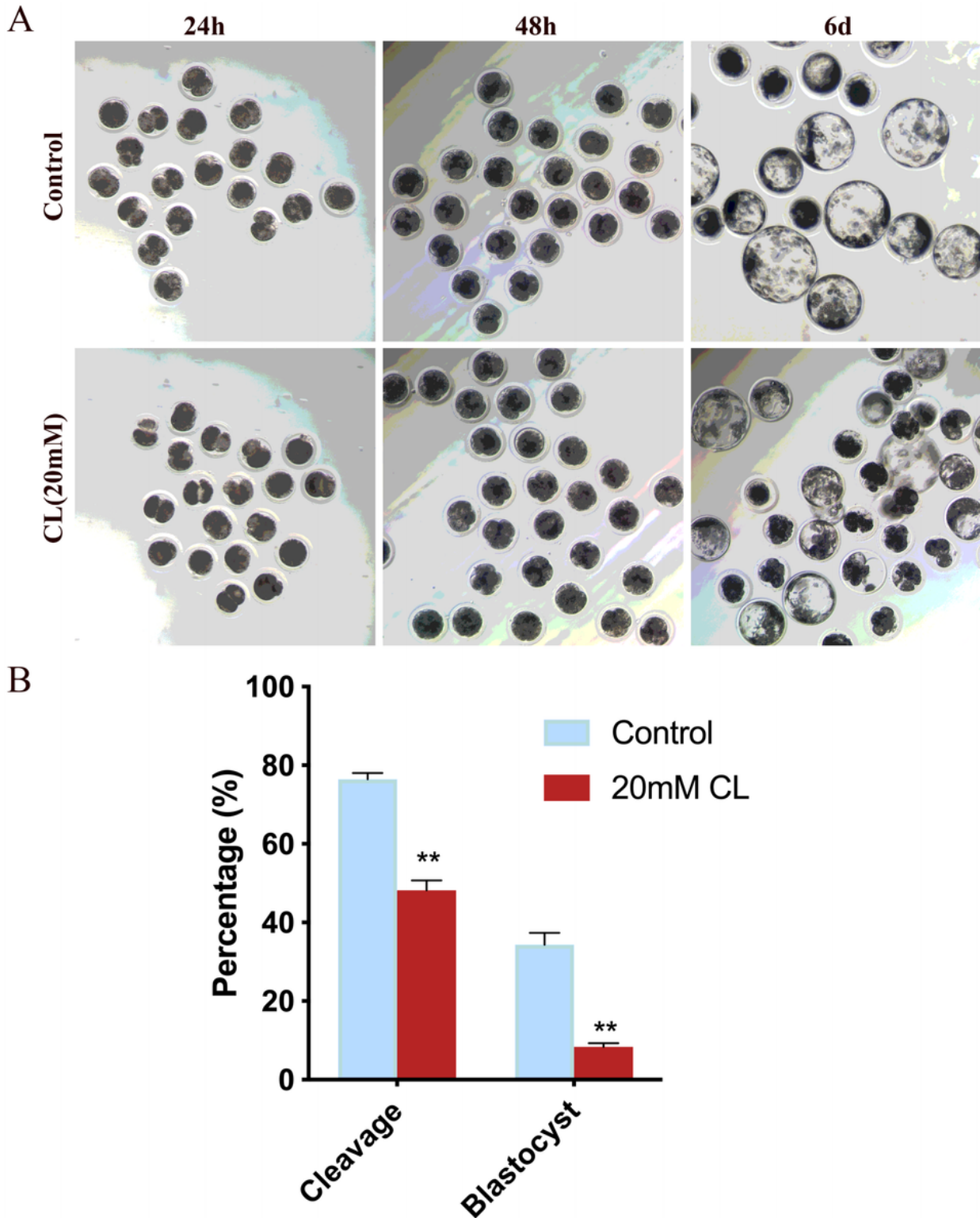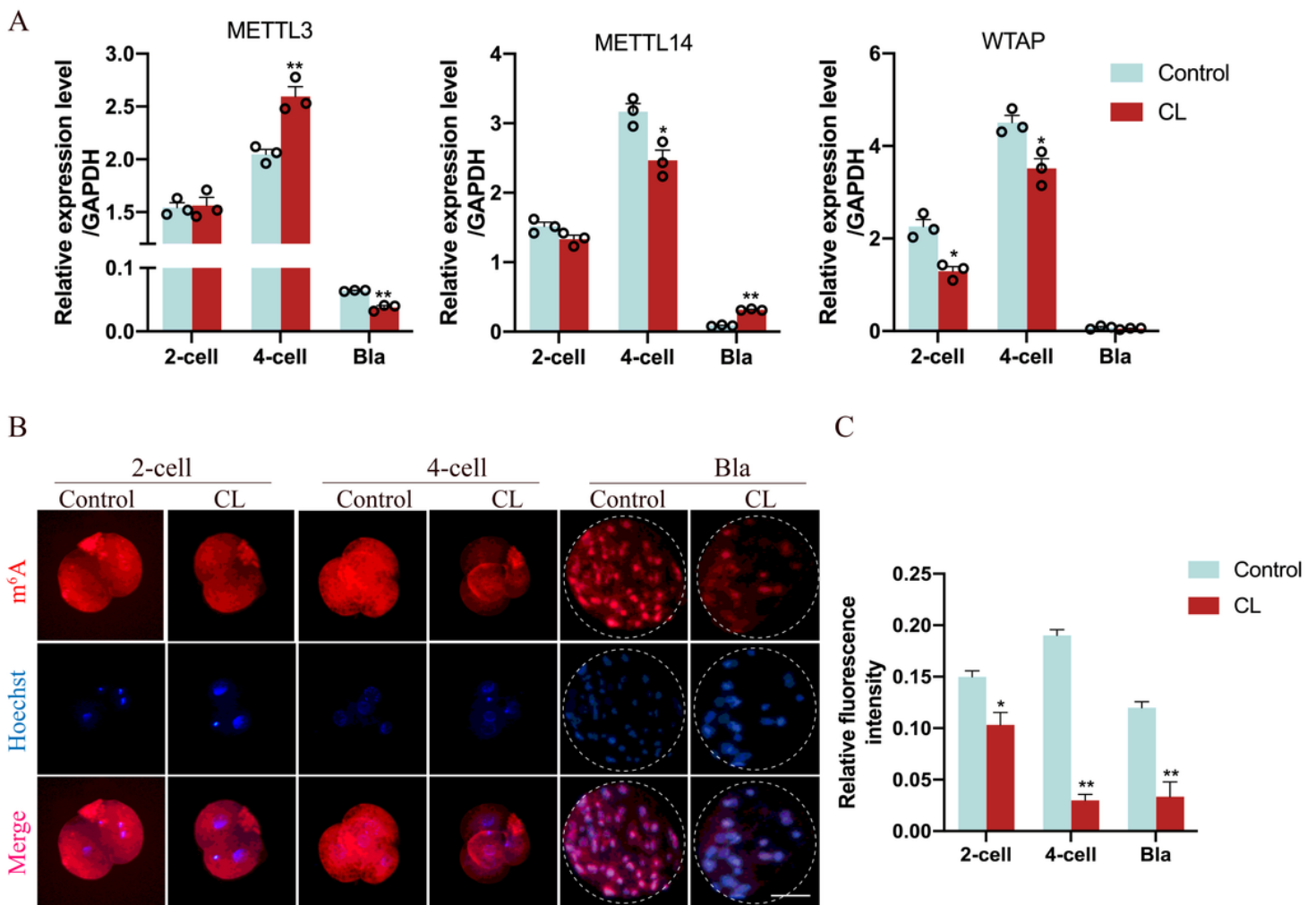

Figure 4

The porcine parthenote development after CL treatment. (a) Representative images of parthenotes taken at 24 h, 48 h and 7 d. Scale bar, 100 μm. (b) The cleavage rates and blastocyst rates of parthenotes were recorded in control and CL-treated groups. Data are expressed as mean ± SEM of three independent experiments. * p < 0.05, ** p < 0.01.

Figure 5

CL treatment decreased the quality of porcine embryos. (a) Representative images of cell apoptosis and (b) DNA damage in blastocysts in control and CL-treated group. Scale bar, 100 μm. (c) The fluorescence intensity of TUNEL and (d) γH2A.X in in blastocysts in control and CL-treated group. (e) Representative images of blastocysts in blastocysts in control and CL-treated group. (f) Representative images of Hoechst staining in blastocysts in two groups. Scale bar, 100 μm. (g) The statistics of diameter and (h) cell number of blastocysts. (i) The relative mRNA expression levels of pluripotency genes (NANOG and OCT4) and apoptosis-related genes (BCL2 and BAX) during porcine embryogenesis. Data are expressed as mean ± SEM of three independent experiments. * p < 0.05, ** p < 0.01.
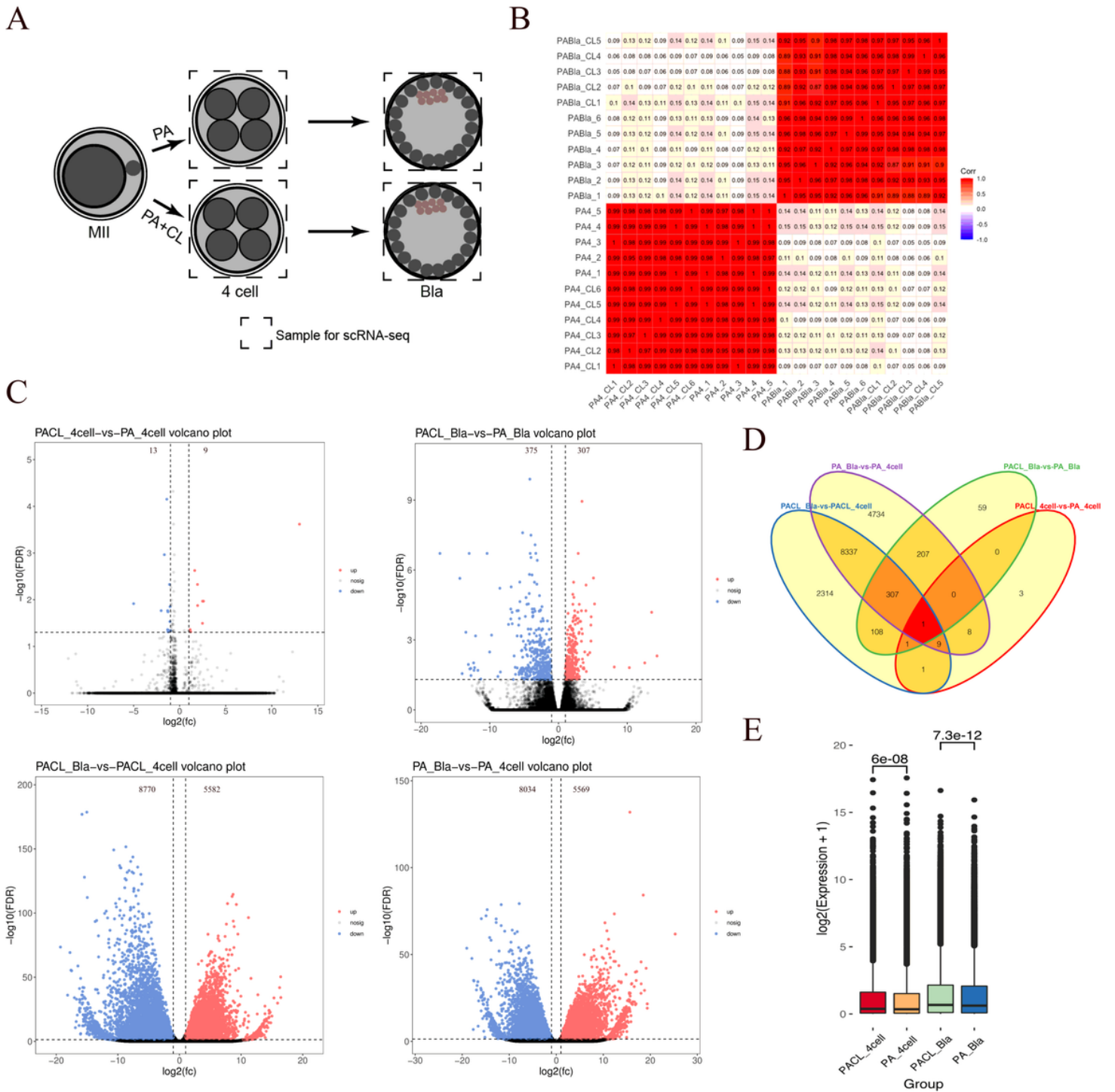

Figure 6

The effect of CL on the levels of nucleic acid methylation. (a) The relative mRNA expression levels of m6A related genes during porcine embryogenesis. (b) Representative images of m6A at different stages of parthenogenetic embryo development in control and CL-treated groups. Scale bar, 100 µm. (c) The fluorescence intensity of m6A. Data are expressed as mean ± SEM of three independent experiments. * p < 0.05, ** p < 0.01.

Figure 7

Histone modifications were differentially affected by CL exposure. (a) Representative images of H3K9me3, (c) H3K4me3 and (e) H4K16ac at different stages of parthenogenetic embryo development in control and CL-treated groups. Scale bar, 100 µm. (b) The fluorescence intensity of H3K9me3, (d) H3K4me3 and (f) H4K16ac. Data are expressed as mean ± SEM of three independent experiments. * p < 0.05, ** p < 0.01.
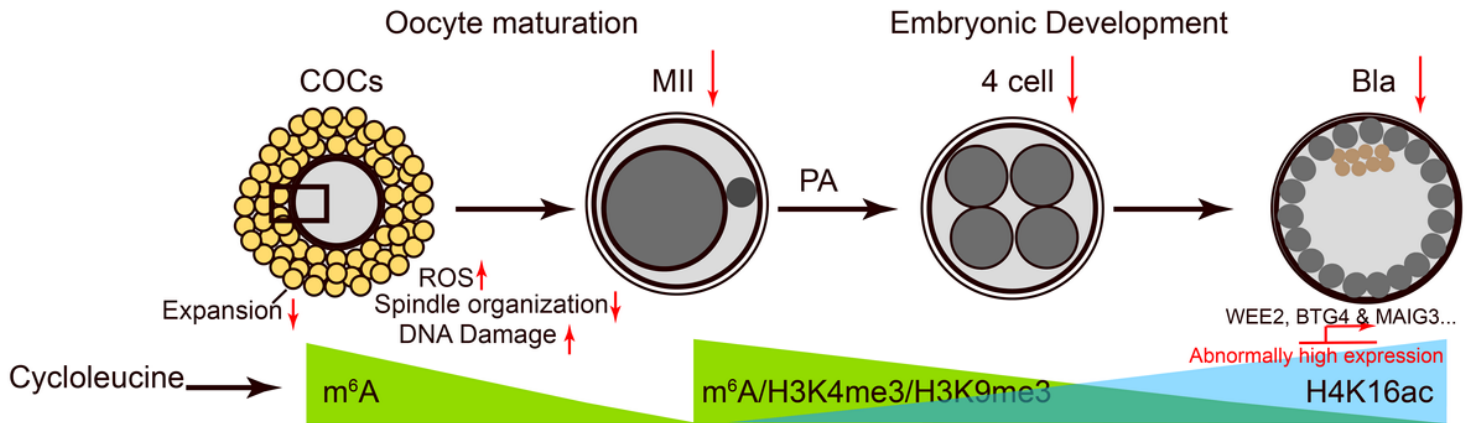
Figure 8

CL exposure altered the global mRNAs expression patterns during porcine embryogenesis. (a) Experimental procedure of scRNA-seq in the present study. (b) The correlation analysis between samples of scRNA-seq. (c) The volcano plots of DE genes between different groups. (d) Venn diagrams of DE genes among four contrasts. (e) The global transcription levels of four groups.

Figure 9

CL exposure altered the global lncRNAs expression patterns during porcine embryogenesis. (a) The fold changes (left Y axis) and number of potential m6A sites (right Y axis) of the top 12 most abundantly DE genes between control and CL-treated blastocysts. (b) The KEGG pathway enrichment analysis of DE genes between PABla and PACL_Bla groups. (c) The volcano plots of DE lncRNAs between different groups. (d-e) The correlation analysis between the expression levels of DE genes and lncRNAs. (f) The lncRNAs-genes network at 4-cell and blastocyst stages.

Figure 10

The model of Cycloleucine (CL) impairs porcine oocyte maturation and early embryonic development via reducing m6A and modulating histone modifications. Briefly, CL decreases porcine oocyte maturation via reducing m6A level thus impairing CCs expansion, ROS levels, DNA damage, spindle/chromosome structure and oocyte maturation. Moreover, CL decreased nucleic acid methylation, H3K9me3, H3K4me3 level while increased acetylation of H4K16 during embryonic development, these changes of epigenetic modifications resulted in abnormally high expression of some maternal genes at blastocyst stages thereby affecting embryonic development.

Supplementary Files

This is a list of supplementary files associated with this preprint. Click to download.

- TableS1.xlsx